HHS Public Access

Author manuscript

Toxicol Appl Pharmacol. Author manuscript; available in PMC 2021 July 01.

Published in final edited form as:

Toxicol Appl Pharmacol. 2020 July 01; 398: 115012. doi:10.1016/j.taap.2020.115012.

Crotonaldehyde-induced Vascular Relaxation and Toxicity: Role of Endothelium and Transient Receptor Potential Ankyrin-1 (TRPA1)

L. Jin[1,2,3,4,5], **G. Jagatheesan**[3,4,5], **J. Lynch**[2,3,4,5], **L. Guo**[3,4,5], **D.J. Conklin**[2,3,4,5,*]

[1]Department of Anesthesiology, Critical Care and Pain Medicine, The Second Affiliated Hospital and Yuying Children's Hospital of Wenzhou Medical University, Wenzhou, China

[2]Department of Pharmacology and Toxicology, School of Medicine, University of Louisville, Louisville, KY USA

[3]Christina Lee Brown Envirome Institute, University of Louisville, Louisville, KY USA

[4]Diabetes and Obesity Center, University of Louisville, Louisville, KY USA

[5]American Heart Association-Tobacco Regulation Center, University of Louisville, Louisville, KY USA

Abstract

Introduction: Crotonaldehyde (CR) is an electrophilic α,β-unsaturated aldehyde present in foods and beverages and is a minor metabolite of 1,3-butadiene. CR is a product of incomplete combustion, and is at high levels in smoke of cigarettes and structural fires. Exposure to CR has been linked to cardiopulmonary toxicity and cardiovascular disease.

Objective: The purpose of this study was to examine the direct effects of CR in murine blood vessels (aorta and superior mesenteric artery, SMA) using an in vitro system.

Methods and Results: CR induced concentration-dependent (1–300 μM) relaxations (75–80%) in phenylephrine (PE) precontracted aorta and SMA. Because the SMA was 20x more sensitive to CR than aorta (SMA EC_{50} 3.8±0.5 μM; aorta EC_{50} 76.0±2.0 μM), mechanisms of CR relaxation

*Correspondence: Daniel J. Conklin, Ph.D., 580 S. Preston St., Delia Baxter Building, Rm. 404E, Diabetes and Obesity Center, University of Louisville, Louisville, KY 40202, Tel: (502) 852-5836, dj.conklin@louisville.edu.

Author contributions

LJ and DC planned, conducted the experiments, generated, analyzed and interpreted data, and wrote the manuscript. GJ, JL, and LG generated data and edited the manuscript. DC is the guarantor of this work. As such, he had full access to all data and takes responsibility for the integrity and accuracy of the data.

Declaration of interests

☒ The authors declare that they have no known competing financial interests or personal relationships that could have appeared to influence the work reported in this paper.

☐ The authors declare the following financial interests/personal relationships which may be considered as potential competing interests:

Conflict of Interest Statement

The authors declare that they have no conflicts of interest with the contents of this article.

were studied in SMA. The CR-induced relaxation at low concentrations (1–30 μM) was inhibited by: 1) mechanically-impaired endothelium; 2) Nω-Nitro-L-arginine methyl ester hydrochloride (L-NAME); 3) guanylyl cyclase (GC) inhibitor (ODQ); 4) transient receptor potential ankyrin-1 (TRPA1) antagonist (A967079); and, 5) by non-vasoactive level of nicotine (1 μM). Similarly, a TRPA1 agonist, allyl isothiocyanate (AITC; mustard oil), stimulated SMA relaxation dependent on TRPA1, endothelium, NO, and GC. Consistent with these mechanisms, TRPA1 was present in the SMA endothelium. CR, at higher concentrations (100–300 μM), induced tension oscillations (spasms) and irreversibly impaired contractility (a vasotoxic effect enhanced by impaired endothelium).

Conclusions: CR relaxation depends on a functional endothelium and TRPA1, whereas vasotoxicity is enhanced by endothelium dysfunction. Thus, CR is both vasoactive and vasotoxic along a concentration continuum.

Graphical Abstract:

Cartoon depicting the mechanisms of CR-induced relaxation in SMA. A) CR induced both vasorelaxation at low concentrations and impaired contractility and triggered spasms at high concentrations in SMA. **B**) Th mechanism or relaxation (**#1**) appeared to start with the activation of the Transient Receptor Potential Ankyrin 1 (TRPA1) cation channels in the endothelium. This step was blocked by a TRPA1 inhibitor (A967079) and SMA from TRPA1-null mice. Calcium entry into endothelial cells enhanced eNOS and NO production. The latter was blocked by NOS inhibition (L-NAME) and endothelial cell impairment (air perfusion). NO released from endothelial cells diffused into vascular smooth muscle cells (VSMC) and activated guanylyl cyclase (GC) to stimulate cGMP formation. This step was blocked by the GC inhibitor (ODQ). We inferred that cGMP activated Protein Kinase G – a known activator of K^+ channel opening in VSMC leading to hyperpolarization, closure of voltage-gated Ca^{++} channels, and relaxation. A second pathway (**#2**) of relaxation must exist because CR relaxed SMA even in the presence of all inhibitors used and mechanical endothelium disruption. The mechanism of this pathway may have involved closure of VSMC Ca^{++} channels because CR relaxed PE-precontracted aorta in a TRPA1-independent manner. The role of VSMC-localized TRPA1 (?) remains to be determined.

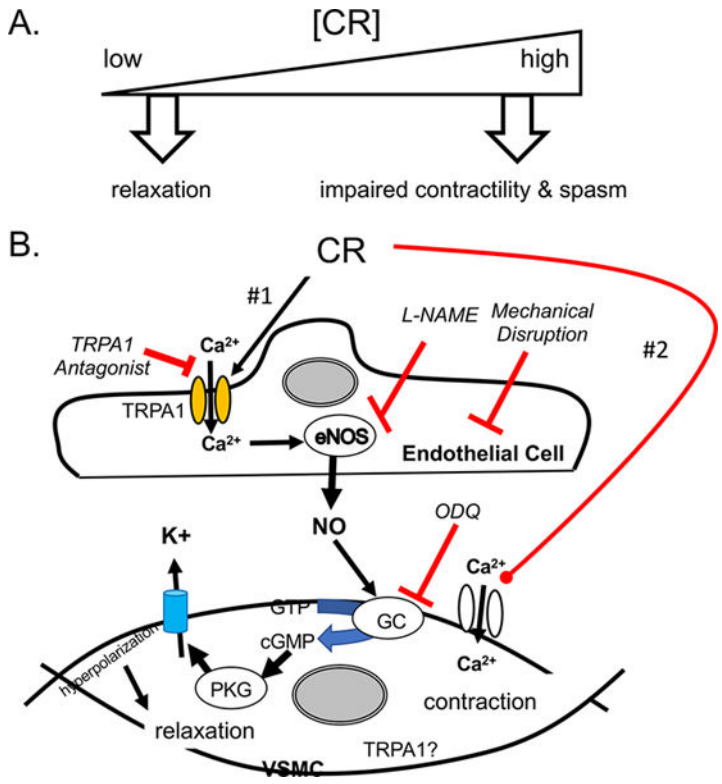

Keywords

aldehydes; crotonaldehyde (CR); transient receptor potential ankyrin-1 (TRPA1); EDRF; mesenteric artery; nitric oxide (NO)

Introduction

Crotonaldehyde (CR) is a highly reactive α,β-unsaturated aldehyde that is environmentally ubiquitous, e.g., found in foods such as fish, meat, fruits and vegetables and beverages, e.g., wine and whiskey (IARC., 1995; Eder *et al.*, 1999). Additional sources of CR exposure include mainstream and side-stream tobacco smoke (IARC., 1995). CR is also formed endogenously during lipid peroxidation (Duescher and Elfarra, 1993; Chung *et al.*, 1996; Chung *et al.*, 1999; Filser *et al.*, 2001; Kawaguchi-Niida *et al.*, 2006; Nair *et al.*, 2007; Voulgaridou *et al.*, 2011), and through the metabolism of 1,3-butadiene (Duescher and Elfarra, 1993; Filser *et al.*, 2001) and metabolism of N-nitrosopyrrolidine (Wang *et al.*, 1988; Hecht *et al.*, 1999). CR can also be formed from acetaldehyde by aldol condensation and dehydration (Tuma *et al.*, 1991). CR is also an important industrial chemical used in the synthesis of tocopherols, sorbitol, and 3-methylbutanol, but it is also a contaminant and a byproduct of various chemical processes (IARC., 1995).

CR can rapidly penetrate cell membranes and induce adverse biological effects, such as inflammation in alveolar macrophages of smokers (Facchinetti *et al.*, 2007; Yang *et al.*, 2013a; Yang *et al.*, 2013b); oxidative stress and apoptosis in epithelial cells (Liu *et al.*,

2010a; Liu *et al.*, 2010b); and toxicity to respiratory tract tissues (Reddy *et al.*, 2002). Glutathione S-transferase P (GSTP) accelerates metabolism of short chain unsaturated aldehydes such as acrolein (3-C) and CR (4-C) via conjugation with glutathione (GSH) (Berhane *et al.*, 1994; Conklin *et al.*, 2015). The major metabolite of CR and a urinary biomarker of CR exposure is 3-hydroxy-1-methylpropyl mercapturic acid (HPMMA) (Gray and Barnsley, 1971). Urinary levels of HPMMA are significantly increased after cigarette smoking and are significantly higher (3x) in U.S. cigarette smokers than in non-smokers (Jain, 2015; Lorkiewicz *et al.*, 2019). Moreover, levels of both HPMMA and 3-hydroxypropyl mercapturic acid (3HPMA; major metabolite of acrolein) are similar in smokers yet as well as in non-smokers, indicating that similar levels of these two aldehydes are found in the environment, derived from endogenous metabolic processes and in cigarette smoke (Jain, 2015).

CR is chemically similar to acrolein, and thus, the lung toxicity of cigarette smoke has been attributed in part to both acrolein and CR. It has been listed as one of nine constituents recommended for disclosure and monitoring by the World Health Organization (WHO) study group on tobacco product regulation (Haussmann, 2012). Moreover, because the primary acrolein metabolite, 3HPMA, is associated with cardiovascular and pulmonary disease risk (DeJarnett et al., 2014; Srivastava et al., 2011; Zhang et al., 2018), it is expected that CR also contributes to disease risk. Similarly, occupational exposure to 1,3-butadiene, a precursor of CR, is associated with cardiovascular disease (Divine, 1990; Matanoski *et al.*, 1990), and in an animal model, exposure to 1,3-butadiene increases arteriosclerotic plaque development in cockerels (Penn and Snyder, 1996). Nonetheless, little research has been dedicated to assess the direct vascular effects of CR.

Because CR and acrolein are known to activate the transient receptor potential ankyrin 1 (TRPA1) channel and because TRPA1 is present in the vasculature, we explored the TRPA1-dependence of CR vasoreactivity in isolated blood vessels (Jin et al., 2019a). TRPA1 is widely distributed in the nervous and cardiovascular systems especially sensory neurons (unmyelinated C-fibers) (Nagata *et al.*, 2005; Anand *et al.*, 2008), endothelial cells (Earley *et al.*, 2009), and heart and cardiomyocytes (Andrei *et al.*, 2016; Conklin *et al.*, 2019). Activation of TRPA1 by a variety of agonists including acrolein, CR and allyl isothiocyanate (AITC, mustard oil) leads to pain (Trevisan *et al.*, 2016), neurogenic tissue inflammation (Schwartz *et al.*, 2011), pulmonary edema and airway hyper-reactivity (Andre *et al.*, 2008; Conklin *et al.*, 2016), vasodilation (Jin *et al.*, 2019a) and hypotension (Pozsgai *et al.*, 2010; Earley, 2012). Thus, TRPA1 may be important in the vasoactive effects of CR.

Consistent with our hypothesis, our research showed that CR induced a significant, concentration-dependent relaxation in superior mesenteric artery (SMA) that was dependent on: 1) a functional endothelium; 2) nitric oxide (NO) formation; 3) guanylyl cyclase (GC); and, 4) TRPA1 activation. High concentrations of CR, however, led to tension oscillations (spasms) and irreversible suppression of contractility (vasotoxicity) without affecting endothelial-dependent function. These data indicate that CR is vasoactive with TRPA1 at low concentrations and vasotoxic at high concentrations.

Material and Methods

Chemicals.

Reagent grade chemicals were purchased from Sigma-Aldrich or other commercial sources as indicated: A967079 (TRPA1 antagonist; AdooQ; Irvine, CA); acetylcholine chloride (ACh); *trans*-crotonaldehyde (CR; 99%); allyl isothiocyanate (AITC, mustard oil); 1h-[1,2,4]oxadiazolo[4,3-a]quinoxalin-1-one (ODQ); N^{ω}-nitro-$_{L}$-arginine methyl ester hydrochloride (L-NAME); L-phenylephrine hydrochloride (PE); sodium nitroprusside (SNP); nicotine bitartrate; and, Ezatiostat (GSTP inhibitor; TLK 199).

Animals.

Male or female wild type C57BL/6J (WT), TRPA1-null and GSTP-null mice (12–20 weeks old; 25–35g) were purchased (The Jackson Laboratory, Bar Harbor, ME) or from in house breeding (Conklin *et al.*, 2009b; Conklin *et al.*, 2017). Mice were treated according to American Physiological Society *Guiding Principles in the Care and Use of Animals*, and all protocols were approved by University of Louisville Institutional Animal Care and Use Committee. Mice were housed under pathogen-free conditions in the University of Louisville vivarium under controlled temperature and 12h light:12h dark cycle. Mice were provided water and a standard chow diet *ad libitum* (Rodent Diet 5010, 4.5% fat by weight, LabDiet; St. Louis, MO).

Estimation of CR Blood Levels: Basal and Post-Mainstream Cigarette Smoke (MCS).

Because there are no available data on blood levels of CR in any animal species, published data of the urinary excretion of the major metabolite of CR (i.e., HPMMA) in mice exposed to air (baseline level) or to mainstream cigarette smoke (MCS; i.e., 50% of smoke from 12 cigarettes over 6h) was used to estimate potential blood levels of CR (Conklin *et al.*, 2018). These data (Fig. 1A) provide an index of ‘CR exposure burden,’ and serve as a basis for justifying the use of CR over a broad concentration range *in vitro*.

CR-Induced Vasoreactivity in Isolated Aorta and Superior Mesenteric Artery (SMA) Isolation and Organ Bath Conditions.

After removal and cleaning of the aorta and SMA, thoracic aorta rings (3–4 mm) were hung on stainless steel hooks in organ baths and SMA rings (2 mm) were hung on tungsten wire in 5-ml heated organ baths (MultiWire Myograph System 620M, DMT, Denmark) in Krebs physiological salt solution (PSS) bubbled with 95% O_2:5% CO_2 at 37 °C. After 10 min without tension, aorta and SMA rings were equilibrated to respective loading tension over 30 min (aorta, 1g; SMA, 0.25g). All rings were stimulated with High K^+ (60 mM) to test for viability, washed 3 times with PSS over 30 min, and re-equilibrated to appropriate resting tension and stimulated again with High K^+ (Jin *et al.*, 2019a) (Schematic). PSS for SMA was (in mM): NaCl, 119; KCl, 4.7; $CaCl_2$, 2.0; $MgCl_2$, 1.2; KH_2PO_4, 1.2; $NaHCO_3$, 24; glucose, 7.0; pH 7.4. PSS for aorta was (in mM): NaCl, 119; KCl, 4.7; $CaCl_2$, 1.6; KH_2PO_4, 1.2; $MgSO_4$, 1.2; $NaHCO_3$, 25; glucose, 5.5; pH 7.4. High K^+ PSS (High K^+; 60 mM) substituted equimolar K^+ for Na^+ in PSS.

Crotonaldehyde (CR) Experimental Series:

CR-Induced Responses. CR (1, 3, 10, 30, 100, and 300 μM) was cumulatively added to organ baths containing either uncontracted or phenylephrine pre-contracted (PE, 10 μM) aorta and SMA (general protocols are in Schematic 1). Isometric tension (mN) developed after first PE addition was "PE_1." The tension (mN) developed after the second PE addition was "PE_2." The tension (mN) developed after the third PE addition was "PE_3." Following exposure to CR, PSS in organ baths was exchanged (3x) with fresh PSS over 30 min, and blood vessels again were precontracted with PE. In uncontracted blood vessels, contractility was quantified as the ratio of PE_2 to PE_1 but also as PE_3 to PE_1 tension (i.e., PE_2/PE_1*100 and PE_3/PE_1*100) (Schematic 1A). In PE-precontracted blood vessels, post-CR contractility was quantified as PE_2 tension to PE_1 tension (i.e., PE_2/PE_1*100) (Schematic 1B). In both settings, PE_2 contractions were relaxed with ACh (10 μM) to test for potential impairment of endothelium-dependent relaxations (Schematic 1).

The efficacy of CR-induced relaxation was calculated as the % reduction in agonist-induced contraction. The sensitivity of CR-induced relaxation was the effective concentration producing 50% response (EC_{50}), i.e., cumulative concentration responses normalized to 100% with interpolation of EC_{50} (Jin *et al.*, 2019a). EC_{50} values were calculated only if the total relaxation as % exceeded 50% of PE_1-induced tension. Exposure to a high CR concentration (300 μM) also induced tension oscillations (spasms) that were quantified by frequency (oscillations/min), amplitude (mN), and duration (s), in part, as previously described (Conklin *et al.*, 2001).

Role of the Endothelium, Nitric Oxide Synthase (NOS), and cGMP.

The role of the endothelium in CR-induced vasorelaxation was studied in SMA with intact and injured endothelium. The endothelium was mechanically injured by air perfusion and damage confirmed by near complete abolition (>95%) of ACh-induced dilation of PE pre-contracted SMA (Jin *et al.*, 2019a). To evaluate the role of NOS, L-NAME (100 μM) was added after addition of PE (10 μM; 15 min) and the plateau of tension (PE_1), and the pre-contracted SMA were then relaxed with cumulative concentrations of CR (1–300 μM). To assess whether cGMP was involved in CR-induced vasorelaxation, PE-precontracted SMA were exposed to ODQ (3 μM; 10 min), to inhibit guanylyl cyclase (GC) activity and the subsequent formation of cGMP (Jiang *et al.*, 2015), followed by cumulative addition of CR (1–300 μM).

Role of TRPA1.

The role of the TRPA1 channel was assessed by incubation of SMA with TRPA1 antagonist (A967079, 1 μM) followed by cumulative addition of CR (1–300 μM). Similarly, effects of CR in SMA of TRPA1-null mice were measured with and without the TRPA1 antagonist (A967079, 1 μM) present. Likewise, the vascular effects of a known TRPA1 agonist, allyl isothiocyanate (AITC, 1–100 μM), were measured in PE-precontracted SMA.

Role of GSTP on CR Relaxation.

Because CR is primarily metabolized by glutathione S-transferase P (GSTP) (Berhane *et al.*, 1994), we assessed whether either genetic deficiency in GSTP or a specific GSTP inhibitor

(Ezatiostat, aka TLK199) may enhance the effects of CR in isolated blood vessels. SMA were PE-precontracted, Ezatiostat (1 μM) was added, and then followed by increasing concentrations of CR (1–300 μM) as described above.

Role of Nicotine.

In users of combustible tobacco, CR and nicotine exposures occur simultaneously, so the direct effects of nicotine on CR were tested. The plateau concentration of nicotine in the blood of smokers throughout the day averages 40 μg/L [0.25 μM] (Moyer *et al.*, 2002) and peak nicotine blood levels encountered by smokers have been 100 μg/L [0.625 μM] (Gourlay and Benowitz, 1997). Thus, we tested the effects of nicotine (1 μM) on CR-induced effects in PE pre-contracted SMA.

TRPA1 Immunofluorescence.

Glass slides with sections (4 μm) of formalin-fixed, paraffin-embedded SMA, aorta and dorsal root ganglia (DRG; positive control) of WT mice were stained with antibodies for immunofluorescence. For immunofluorescence, slides with either cross sections of blood vessels or DRG were stained with a rabbit polyclonal TRPA1-specific antibody (1:200; Alomone Labs, Israel; Cat. #: ACC-037). The fluorophore used was Alexa Fluor 647 tagged goat anti-rabbit secondary antibody (1:400 dilution; Invitrogen; Cat. #: 21244) with or without a TRPA1 blocking peptide (see Conklin et al., 2019). To stain cell nuclei, sections were coated with DAPI containing Slow Fade® Gold anti-fade reagent (Invitrogen; Cat. #: S36938). Fluorescence imaging was done using a Nikon eclipse Ti fluorescence microscope using NIS-Elements (Nikon; Japan) at 200X. Two filters were used for TRPA1 (Cy5 Red filter) and nuclear (DAPI filter) staining, respectively (Conklin *et al.*, 2019; Jin *et al.*, 2019a). To specifically label endothelial cells, blood vessel sections were co-stained with isolectin GS-IB4 Alexa Fluor 594 conjugate (1:200 dilution; Invitrogen; Cat. #: I21413) – an endothelial cell-specific marker -- and with TRPA1 antibody (as described).

Histology.

After immunofluorescence was performed, g lass slides with sections (4 μm) of formalin-fixed, paraffin-embedded SMA, aorta and dorsal root ganglia (DRG; positive control) of WT mice were stained with hematoxylin and eosin (H&E) to show normal histological structures for reference. Images of H&E-stained sections were taken using a digital Spot camera mounted on an Olympus microscope.

Statistical Analyses.

Data are expressed as means ± SE. When comparing two groups, a *t*-test was used (paired or unpaired as appropriate). Multiple group testing was done with One-Way ANOVA with Bonferroni post hoc. If either equal variance or normality test failed, One-Way ANOVA on Ranks (Kruskal-Wallis) and Dunn’s post hoc was used (SigmaPlot, ver. 12). Statistical significance was assumed where $p<0.05$.

Results

Urinary CR Metabolite, HPMMA, is Elevated in Mice Exposed to Mainstream Cigarette Smoke (MCS).

The total urinary HPMMA (μg) excreted from C57BL/6 (WT) mice after exposure to MCS of KY Reference cigarettes (3R4F) was increased approximately 2.7x compared with HPMMA in urine of air-exposed mice (Fig. 1A). Urinary nicotine was only present in urine of MCS-exposed mice (Fig. 1A). Baseline excretion of HPMMA (approximately 1.8 μg/16h) is equivalent to 0.025 μmoles of CR (MW = 70.07), and as the blood volume of a 25g mouse is approximately 2 ml, this amount of CR approximates to 12.5 μM in blood. As HPMMA level was increased 2.7x after MCS exposure, a potential blood level of CR >30 μM was estimated. As cigarette smoking can be quite intense (>2 packs a day) and likely leads to high CR exposures, we predict that smoking-related exposures may result in much higher blood CR levels than 30 μM. To encompass this possibility, we tested for the direct vascular effects of CR from 1–300 μM to cover a broad systemic concentration range.

Concentration-Dependent Effects.

In uncontracted SMA, cumulative CR (1–300 μM) had no effect on basal tension (myogenic tone; **data not shown**). In the continued presence of 300 μM CR, PE-induced tension (84.0±12.8% of PE_1; n=3) was slightly impaired (p=0.055) while ACh relaxation was unaffected (−91.1±1.3%; n=3). However, after 3 bath changes of PSS over 30 min, the CR-treated SMA produced only 26.6±15.0% (n=3; p=0.001) of tension of PE_1; yet, it still retained a functional ACh relaxation (−84.6±2.4%; n=3).

In PE-precontracted aorta and SMA, cumulative CR (1–300 μM) induced significant, concentration-dependent relaxations of 75–80% reduction in tension (Fig. 1B & 1C; respectively; Tables 1, 2, Suppl. Table 1). In SMA at CR [300 μM], there was a consistent reversal of relaxation accompanied by tension oscillations (spasms) (Fig. 1B), although no oscillations were observed in aorta (Fig. 1C). The SMA were significantly more sensitive (20x) to CR than aorta (SMA EC_{50} 3.8±0.5 μM; aorta EC_{50} 76.0±2.0 μM; p<0.05) (Fig. 1D; Tables 1–2). The female SMA were statistically less sensitive to CR (SMA EC_{50} 6.6±0.3 μM) than male SMA (Table 2).

CR-induced tension oscillation (spasm) frequency was low (<2/min), of modest amplitude (<2.5 mN) and usually <30 s in duration (Fig. 1B; Table 3). Endothelial impairment abolished CR-induced tension oscillations, and likewise, L-NAME treatment decreased oscillation frequency by 35% and amplitude by 60% although neither reduction was statistically significant (Table 3).

Mechanisms of CR-Induced Vasorelaxation.

The CR-induced relaxation at 1–30 μM was significantly inhibited in PE-pre-contracted WT SMA by a mechanically-disrupted endothelium (>90% loss of ACh-induced relaxation) (Figs. 2A–B; Tables 1–2). Similarly, CR-induced relaxation in PE pre-contracted SMA was equally inhibited in the presence of L-NAME (Figs. 2C–D; Tables 1–2). This L-NAME effect indicated a role of NO (likely eNOS) as critical in the low concentration range of the

CR-induced relaxation in PE-precontracted SMA. Similarly, ODQ treatment, an irreversible guanylyl cyclase (GC) inhibitor, significantly blocked the low concentration range of the CR-induced relaxation (Figs. 2E–F; Tables 1–2).

Role of TRPA1 channel in the CR-induced relaxation.

Because CR is a known agonist of TRPA1, we hypothesized that the TRPA1 channel contributes to endothelium-dependent CR-induced vasorelaxation in SMA. The TRPA1 antagonist, A967079 (1 μM), significantly inhibited the sensitive range (<10 μM) of the CR-induced relaxation in PE-contracted SMA (Fig. 3A–B; Tables 1–2). We also tested CR-induced relaxation with or without A967079 (1 μM) in PE-contracted SMA of male TRPA1-null mice (Fig. 3C–D; Tables 1–2). In contrast, the presence of A967079 appeared to slightly enhance the relaxation of CR in TRPA1-null SMA (Fig. 3D). Because AITC is a known TRPA1 agonist, we tested for concentration- and TRPA1-dependent relaxation in WT SMA. AITC-induced relaxation was inhibited by the TRPA1 antagonist (A976709) (Fig. 3E). Similarly, the AITC relaxation was less sensitive in SMA of TRPA1-null mice than WT mice (Fig. 3F) (see EC_{50}s; Table 2). Unlike CR, however, AITC alone up to 100 μM did not induce tension oscillations (0/5; Fig. 3E).

Because CR is a substrate of GSTP, we tested for a metabolic (detoxification) role of GSTP in SMA. There was no difference in the CR-induced relaxation in PE-contracted SMA of either GSTP-null mice or in WT SMA after addition of the GSTP inhibitor, Ezatiostat (TLK 199), compared with WT SMA (Suppl. Fig. 1A–D; Tables 1–2). GSTP deficiency or GSTP inhibition had no effect on CR-induced tension oscillations (Table 3).

Formalin-fixed, paraffin-embedded, cross-sections of murine WT SMA and aorta were stained with H&E to show normal vascular structure (Fig. 4A,D). In immunofluorescently-stained, cross-sections of WT SMA, positive TRPA1 staining (shown in green; Fig. 4B) was co-localized in the endothelium as indicated by the endothelial cell marker, isolectin (shown in red; overlap of fluorophores = yellow; Fig. 4C). Modest, yet specific TRPA1 staining also was present in the media:adventitia border of SMA (shown in green; Fig. 4B). Although aorta had positive TRPA1 staining localized in the media (shown in green; Fig. 4E), there was no staining observed in the endothelium of aorta. Positive TRPA1 staining was absent when a TRPA1 blocking peptide was present in aorta (Fig. 4F) and in dorsal root ganglion (DRG; Suppl. Fig. 2) sections, which served as a positive control for TRPA1 staining (Conklin *et al.*, 2019).

Impaired Contractility (vasotoxicity) of CR.

The PE_2/PE_1 tension ratio was measured as a metric of impaired contractility after CR exposure and 3 PSS buffer exchanges, and it was significantly decreased after CR exposure compared with the untreated control group (Fig. 5A, Table 4). The PE_2/PE_1 tension ratio was further decreased in both endothelial dysfunction (ED) and ODQ pre-treatment groups compared with the CR only group (Fig. 5A). There were no differences with any other treatment group except the GSTP inhibitor, Ezatiostat, that protected SMA from CR-induced impairment of contractility (Fig. 5A). Although CR depressed PE_2/PE_1 tension, CR had no effect on subsequent ACh-induced relaxation (Fig. 5B, Table 3). No other co-treatment

along with CR affected ACh-induced relaxation excepting the 2 groups that were designed to impair endothelium function: ED and L-NAME treatment (Fig. 5B, Table 4), suggesting that CR did not induce acute endothelial cell injury despite significantly impairing contractility.

Nicotine and CR.

In users of combustible tobacco, CR and nicotine exposures occur simultaneously. Thus, whether nicotine altered CR-induced effects in WT SMA was tested. Nicotine at levels potentially achieved in smokers (1 μM) had no effect on tension in PE-contracted SMA (Suppl. Fig. 3A). In the presence of nicotine, CR-induced vasorelaxation was decreased significantly (Suppl. Fig. 3B; Table 1). Nicotine at supra-pharmacological levels of >10 μM induced relaxation in PE-contracted SMA (Suppl. Fig. 3A).

Discussion

To our knowledge, this is the first study to show the vasoreactivity of CR and its mechanisms of action that include TRPA1 in blood vessels. The mechanisms of CR-induced vasorelaxation are similar to those of formaldehyde, including dependence on TRPA1, endothelium, NO formation and guanylyl cyclase activation (Jin *et al.*, 2019a). The potency and efficacy of CR-induced relaxation in SMA is reminiscent of actions of acrolein in perfused rat mesenteric bed (Awe *et al.*, 2006), isolated rat coronary artery (Conklin *et al.*, 2001) and isolated mouse aorta (Conklin *et al.*, 2009a). Moreover, we show that, as for acrolein (Conklin *et al.*, 2001), CR at higher concentrations induces tension oscillations (spasms) and impairs contractility (vasotoxicity) in SMA (see Graphical Abstract). This continuum from potent relaxation (low concentrations) to vascular toxicant (high concentration) belies the importance of studying these responses as CR is abundant in foods, beverages, occupational settings, and especially, in combustion-derived smoke, i.e., tobacco smoke, wildfires, etc... Thus, appreciating the avidity of unsaturated aldehydes for altering vascular wall function is a first step toward better understanding how exposure to CR may increase cardiovascular disease risk.

Because TRPA1 is shown to be involved with the vascular responses induced by other aldehydes, it was expected that CR may trigger a TRPA1-dependent vasorelaxation. For example, activation of TRPA1 can lead to the release of vasoactive peptides, substance P (SubP) and CGRP (Trevisan *et al.*, 2016) that can induce vasodilation and inflammatory responses (Conklin, 2016; Achanta *et al.*, 2018). The mechanism of CR-induced TRPA1-mediated relaxations in SMA, however, appears dependent largely on endothelium-localized TRPA1, as we show that endothelial impairment either by air perfusion or by L-NAME shifts the sensitivity of the CR response rightward to a degree similar to that of either TRPA1 antagonist treatment or use of TRPA1-null SMA. These data are mirrored by SMA relaxation induced by a TRPA1 agonist AITC that is similarly shifted to the right by both A967079 (TRPA1 inhibitor) and TRPA1 deletion. Nevertheless, we cannot fully rule out that other cells in the isolated SMA, e.g., perivascular nerves, contribute to CR's mechanism of relaxation. Moreover, there are at least 2 mechanisms mediating the full relaxation of CR: 1) endothelium-based; and, 2) time-dependent, irreversible change in vascular smooth muscle

cell (VSMC) contractile machinery, e.g., closure of VSMC calcium channels. Although the latter conclusion has limited experimental support, we infer it because contractility is significantly impaired after CR exposure (and even after removal); endothelial function is intact because ACh-induced relaxation is unaffected post-CR (no endothelium dysfunction); and, previous experience with similar vascular toxicity of acrolein led to findings consistent with a role of external calcium (Conklin *et al.*, 2006).

Cigarette smoke is a major source of exogenous CR (Goniewicz *et al.*, 2017; Lorkiewicz *et al.*, 2019) as well as other aldehydes. We calculate that exposure of mice to MCS increases excretion of the CR metabolite, HPMMA, by 2.7x, indicating that CR is produced endogenously in mice. Our estimation of circulating basal blood levels of CR puts it in the low end of the vasoactive range - a novel consideration. Many unsaturated aldehydes are noted potent vasodilators including acrolein (Awe *et al.*, 2006), 4-hydroxynonenal (4HNE) (Martinez *et al.*, 1994; Romero *et al.*, 1997) and cinnamaldehyde (Yanaga *et al.*, 2006; Pozsgai *et al.*, 2010), and now CR -- all known ligands of TRPA1. These potent dilatory effects may contribute to a variety of physiological processes such as postprandial hyperemia or flow-mediated dilation (FMD) or response to injury/infection. However, too much of any of these aldehydes may lead to pathological changes including vasospasm, atherosclerosis and vascular toxicity (Conklin *et al.*, 2001; Conklin *et al.*, 2006; Boor and Conklin, 2008). High concentrations of CR impair contractility and also stimulate tension oscillations (spasms) in SMA yet neither effect appears dependent on TRPA1 because both effects occur in WT and TRPA1-null SMA and in the presence of a TRPA1 antagonist. Interestingly, endothelial dysfunction worsens impairment of contractility yet prevents spasms, indicating that endothelial-derived factors likely protect VSMC from impairment yet promote spasm.

Although parent unsaturated aldehydes activate TRPA1 via covalent modification intracellular free cysteines of amino-terminus (Macpherson *et al.*, 2007), it is unclear if metabolism of CR alters this mechanism of activation. Interestingly, we did not find evidence that vascular GSTP in SMA (enzyme responsible for metabolism of CR via GSH conjugation and detoxification) alters CR-induced effects despite using 2 approaches: a GSTP-null mouse (genetic deletion) and a GSTP inhibitor (Ezatiostat, TLK199). One explanation is that CR (under our *in vitro* conditions) rapidly inactivates GSTP via active site sulfhydryl conjugation thereby functionally impairing GSTP in WT blood vessels (Iersel *et al.*, 1996) and making comparisons with GSTP-null or GSTP inhibitor mute. Notably, the GSTP inhibitor limits impaired contractility induced by CR (more subtly in GSTP-null) but not the tension oscillations (spasms). A mechanism for this unexpected effect will need to be investigated.

Nicotine is also an important component of tobacco smoke, and nicotine activates the sympathetic nervous system that can increase cardiovascular disease risk factors such as heart rate and blood pressure and decrease heart rate variability (HRV). These changes, in turn, affect myocardial remodeling, impair lipid metabolism, and stimulate inflammation (Dutta *et al.*, 2012; Benowitz and Burbank, 2016). The plateau concentration of nicotine in the blood of smokers throughout the day averages 40 μg/L (0.25 μM) (Moyer *et al.*, 2002), and thus, we tested whether effects of pharmacological level of nicotine (1 μM) could alter

CR effects in PE pre-contracted SMA. Interestingly, nicotine at 1 μM (a non-vasoactive concentration) modestly suppresses CR-induced relaxation. The mechanism of this effect is unclear, but inhaled nicotine at a high concentration (1 mM) is thought to activate sensory TRPA1 channel and stimulate airway constriction reflex (Talavera *et al.*, 2009). Our previous studies show that nicotine (1 μM) presence has no effect on formaldehyde- or acetaldehyde-induced relaxations in PE-contracted SMA (Jin *et al.*, 2019a; Jin *et al.*, 2019b), indicating that this nicotine effect appears specific for CR. Inhibition of CR relaxation may promote the sympathomimetic effects of nicotine alone, e.g., increased blood pressure, perhaps counteracting the depressor effects of CR.

In conclusion, this study describes a sensitive mechanism of CR-induced vasorelaxation that is sequentially dependent on endothelium-localized TRPA1 channel, NO, and a VSMC GC pathway in SMA (but not in aorta), which may play an important role in regulating blood flow/blood pressure at low endogenous levels of CR. At high concentrations (300 μM) of CR, there are smooth muscle impairment and tension oscillations (reminiscent of “spasms” observed with acrolein *in vitro* – another vasotoxic and TRPA1 agonist compound) that appear independent of TRPA1. Future studies of the *in vivo* contribution of CR and TRPA1 to cardiovascular physiology and pathophysiology especially with regard to smoke inhalation (wildfire or tobacco) are required to better understand how exposure to reactive aldehydes confers increased cardiovascular disease risk.

Supplementary Material

Refer to Web version on PubMed Central for supplementary material.

Acknowledgements

The authors thank the University of Louisville Diabetes and Obesity Center for technical support.

Grants

This research was funded by NIH grants: U54HL120163, HL122676, and GM127607.

REFERENCES

Achanta S, Chintagari NR, Brackmann M, Balakrishna S, Jordt SE, 2018 TRPA1 and CGRP antagonists counteract vesicant-induced skin injury and inflammation. Toxicol Lett 293, 140–148. [PubMed: 29535050]

Anand U, Otto WR, Facer P, Zebda N, Selmer I, Gunthorpe MJ, Chessell IP, Sinisi M, Birch R, Anand P, 2008 TRPA1 receptor localisation in the human peripheral nervous system and functional studies in cultured human and rat sensory neurons. Neuroscience letters 438, 221–227. [PubMed: 18456404]

Andre E, Campi B, Materazzi S, Trevisani M, Amadesi S, Massi D, Creminon C, Vaksman N, Nassini R, Civelli M, Baraldi PG, Poole DP, Bunnett NW, Geppetti P, Patacchini R, 2008 Cigarette smoke-induced neurogenic inflammation is mediated by alpha,beta-unsaturated aldehydes and the TRPA1 receptor in rodents. J Clin Invest 118, 2574–2582. [PubMed: 18568077]

Andrei SR, Sinharoy P, Bratz IN, Damron DS, 2016 TRPA1 is functionally co-expressed with TRPV1 in cardiac muscle: Co-localization at z-discs, costameres and intercalated discs. Channels (Austin) 10, 395–409. [PubMed: 27144598]

Awe SO, Adeagbo AS, D'Souza SE, Bhatnagar A, Conklin DJ, 2006 Acrolein induces vasodilatation of rodent mesenteric bed via an EDHF-dependent mechanism. Toxicology and Applied Pharmacology 217, 266–276. [PubMed: 17069868]

Benowitz NL, Burbank AD, 2016 Cardiovascular toxicity of nicotine: Implications for electronic cigarette use. Trends in cardiovascular medicine 26, 515–523. [PubMed: 27079891]

Berhane K, Widersten M, Engstrom A, Kozarich JW, Mannervik B, 1994 Detoxication of base propenals and other alpha, beta-unsaturated aldehyde products of radical reactions and lipid peroxidation by human glutathione transferases. Proc.Natl.Acad.Sci.U.S.A 91, 1480–1484. [PubMed: 8108434]

Boor PJ, Conklin DJ, 2008 The arterial media as a target of structural and functional injury by chemicals In Acosta D, (Ed.), Cardiovascular Toxicology. Informa Healthcare, New York, pp. 667–691.

Chung FL, Chen HJ, Nath RG, 1996 Lipid peroxidation as a potential endogenous source for the formation of exocyclic DNA adducts. Carcinogenesis 17, 2105–2111. [PubMed: 8895475]

Chung FL, Nath RG, Nagao M, Nishikawa A, Zhou GD, Randerath K, 1999 Endogenous formation and significance of 1,N2-propanodeoxyguanosine adducts. Mutat Res 424, 71–81. [PubMed: 10064851]

Conklin DJ, 2016 Acute cardiopulmonary toxicity of inhaled aldehydes: role of TRPA1. Ann N Y Acad Sci 1374, 59–67. [PubMed: 27152448]

Conklin DJ, Bhatnagar A, Cowley HR, Johnson GH, Wiechmann RJ, Sayre LM, Trent MB, Boor PJ, 2006 Acrolein generation stimulates hypercontraction in isolated human blood vessels. Toxicology and Applied Pharmacology 217, 277–288. [PubMed: 17095030]

Conklin DJ, Boyce CL, Trent MB, Boor PJ, 2001 Amine metabolism: a novel path to coronary artery vasospasm. Toxicology and Applied Pharmacology 175, 149–159. [PubMed: 11543647]

Conklin DJ, Guo Y, Jagatheesan G, Nystoriak MA, Obal D, Kilfoil P, Guo L, Hoetker JDH, Bolli R, Bhatnagar A, 2019 Transient Receptor Potential Ankyrin-1 (TRPA1) Channel Contributes to Myocardial Ischemia-Reperfusion Injury. Am J Physiol Heart Circ Physiol.

Conklin DJ, Haberzettl P, Jagatheesan G, Baba S, Merchant ML, Prough RA, Williams JD, Prabhu SD, Bhatnagar A, 2015 Glutathione S-transferase P protects against cyclophosphamide-induced cardiotoxicity in mice. Toxicol Appl Pharmacol 285, 136–148. [PubMed: 25868843]

Conklin DJ, Haberzettl P, Jagatheesan G, Kong M, Hoyle GW, 2016 Role of TRPA1 in acute cardiopulmonary toxicity of inhaled acrolein. Toxicol Appl Pharmacol.

Conklin DJ, Haberzettl P, Jagatheesan G, Kong M, Hoyle GW, 2017 Role of TRPA1 in acute cardiopulmonary toxicity of inhaled acrolein. Toxicol Appl Pharmacol 324, 61–72. [PubMed: 27592100]

Conklin DJ, Haberzettl P, Prough RA, Bhatnagar A, 2009a Glutathione-S-transferase P protects against endothelial dysfunction induced by exposure to tobacco smoke. Am.J.Physiol Heart Circ.Physiol 296, H1586–H1597. [PubMed: 19270193]

Conklin DJ, Haberzettl P, Prough RA, Bhatnagar A, 2009b Glutathione-S-transferase P protects against endothelial dysfunction induced by exposure to tobacco smoke. Am J Physiol Heart Circ Physiol 296, H1586–1597. [PubMed: 19270193]

Conklin DJ, Ogunwale MA, Chen Y, Theis WS, Nantz MH, Fu XA, Chen LC, Riggs DW, Lorkiewicz P, Bhatnagar A, Srivastava S, 2018 Electronic cigarette-generated aldehydes: The contribution of e-liquid components to their formation and the use of urinary aldehyde metabolites as biomarkers of exposure. Aerosol Sci Technol 52, 1219–1232. [PubMed: 31456604]

Divine BJ, 1990 An update on mortality among workers at a 1,3-butadiene facility--preliminary results. Environ Health Perspect 86, 119–128. [PubMed: 2401252]

Duescher RJ, Elfarra AA, 1993 Chloroperoxidase-mediated oxidation of 1,3-butadiene to 3-butenal, a crotonaldehyde precursor. Chem Res Toxicol 6, 669–673. [PubMed: 8292745]

Dutta P, Courties G, Wei Y, Leuschner F, Gorbatov R, Robbins CS, Iwamoto Y, Thompson B, Carlson AL, Heidt T, Majmudar MD, Lasitschka F, Etzrodt M, Waterman P, Waring MT, Chicoine AT, van der Laan AM, Niessen HW, Piek JJ, Rubin BB, Butany J, Stone JR, Katus HA, Murphy SA, Morrow DA, Sabatine MS, Vinegoni C, Moskowitz MA, Pittet MJ, Libby P, Lin CP, Swirski FK,

Weissleder R, Nahrendorf M, 2012 Myocardial infarction accelerates atherosclerosis. Nature 487, 325–329. [PubMed: 22763456]

Earley S, 2012 TRPA1 channels in the vasculature. Br J Pharmacol 167, 13–22. [PubMed: 22563804]

Earley S, Gonzales AL, Crnich R, 2009 Endothelium-dependent cerebral artery dilation mediated by TRPA1 and Ca2+-Activated K+ channels. Circ Res 104, 987–994. [PubMed: 19299646]

Eder E, Schuler D, Budiawan, 1999 Cancer risk assessment for crotonaldehyde and 2-hexenal: an approach. IARC scientific publications, 219–232. [PubMed: 10626223]

Facchinetti F, Amadei F, Geppetti P, Tarantini F, Di Serio C, Dragotto A, Gigli PM, Catinella S, Civelli M, Patacchini R, 2007 Alpha, beta-unsaturated aldehydes in cigarette smoke release inflammatory mediators from human macrophages. Am J Respir Cell Mol Biol 37, 617–623. [PubMed: 17600310]

Filser JG, Faller TH, Bhowmik S, Schuster A, Kessler W, Putz C, Csanady GA, 2001 First-pass metabolism of 1,3-butadiene in once-through perfused livers of rats and mice. Chem Biol Interact 135–136, 249–265.

Goniewicz ML, Gawron M, Smith DM, Peng M, Jacob P 3rd, Benowitz NL, 2017 Exposure to Nicotine and Selected Toxicants in Cigarette Smokers Who Switched to Electronic Cigarettes: A Longitudinal Within-Subjects Observational Study. Nicotine Tob Res 19, 160–167. [PubMed: 27613896]

Gourlay SG, Benowitz NL, 1997 Arteriovenous differences in plasma concentration of nicotine and catecholamines and related cardiovascular effects after smoking, nicotine nasal spray, and intravenous nicotine. Clin Pharmacol Ther 62, 453–463. [PubMed: 9357397]

Gray JM, Barnsley EA, 1971 The metabolism of crotyl phosphate, crotyl alcohol and crotonaldehyde. Xenobiotica 1, 55–67. [PubMed: 4356091]

Haussmann HJ, 2012 Use of hazard indices for a theoretical evaluation of cigarette smoke composition. Chem Res Toxicol 25, 794–810. [PubMed: 22352345]

Hecht SS, Upadhyaya P, Wang M, 1999 Reactions of alpha-acetoxy-N-nitrosopyrrolidine and crotonaldehyde with DNA. IARC scientific publications, 147–154. [PubMed: 10626216]

IARC., 1995 Crotonaldehyde. International Agency of Research on Cancer.

Iersel ML, Ploemen JP, Struik I, van AC, Keyzer AE, Schefferlie JG, van Bladeren PJ, 1996 Inhibition of glutathione S-transferase activity in human melanoma cells by alpha,beta-unsaturated carbonyl derivatives. Effects of acrolein, cinnamaldehyde, citral, crotonaldehyde, curcumin, ethacrynic acid, and trans-2-hexenal. Chemico-Biological Interactions 102, 117–132. [PubMed: 8950226]

Jain RB, 2015 Distributions of selected urinary metabolites of volatile organic compounds by age, gender, race/ethnicity, and smoking status in a representative sample of U.S. adults. Environ Toxicol Pharmacol 40, 471–479. [PubMed: 26282484]

Jiang M, Wan F, Wang F, Wu Q, 2015 Irisin relaxes mouse mesenteric arteries through endothelium-dependent and endothelium-independent mechanisms. Biochem Biophys Res Commun 468, 832–836. [PubMed: 26582714]

Jin L, Jagatheesan G, Guo L, Nystoriak M, Malovichko M, Lorkiewicz P, Bhatnagar A, Srivastava S, Conklin DJ, 2019a Formaldehyde Induces Mesenteric Artery Relaxation via a Sensitive Transient Receptor Potential Ankyrin-1 (TRPA1) and Endothelium-Dependent Mechanism: Potential Role in Postprandial Hyperemia. Front Physiol 10, 277. [PubMed: 30984013]

Jin L, Lorkiewicz P, Malovichko MV, Bhatnagar A, Srivastava S, Conklin DJ, 2019b Acetaldehyde Induces an Endothelium-Dependent Relaxation of Superior Mesenteric Artery: Potential Role in Postprandial Hyperemia. Front Physiol 10, 1315. [PubMed: 31695624]

Kawaguchi-Niida M, Shibata N, Morikawa S, Uchida K, Yamamoto T, Sawada T, Kobayashi M, 2006 Crotonaldehyde accumulates in glial cells of Alzheimer's disease brain. Acta Neuropathol 111, 422–429. [PubMed: 16538519]

Liu XY, Yang ZH, Pan XJ, Zhu MX, Xie JP, 2010a Crotonaldehyde induces oxidative stress and caspase-dependent apoptosis in human bronchial epithelial cells. Toxicol Lett 195, 90–98. [PubMed: 20153411]

Liu XY, Yang ZH, Pan XJ, Zhu MX, Xie JP, 2010b Gene expression profile and cytotoxicity of human bronchial epithelial cells exposed to crotonaldehyde. Toxicol Lett 197, 113–122. [PubMed: 20471460]

Lorkiewicz P, Riggs DW, Keith RJ, Conklin DJ, Xie Z, Sutaria S, Lynch B, Srivastava S, Bhatnagar A, 2019 Comparison of Urinary Biomarkers of Exposure in Humans Using Electronic Cigarettes, Combustible Cigarettes, and Smokeless Tobacco. Nicotine Tob Res 21, 1228–1238. [PubMed: 29868926]

Macpherson LJ, Dubin AE, Evans MJ, Marr F, Schultz PG, Cravatt BF, Patapoutian A, 2007 Noxious compounds activate TRPA1 ion channels through covalent modification of cysteines. Nature 445, 541–545. [PubMed: 17237762]

Martinez MC, Bosch-Morell F, Raya A, Roma J, Aldasoro M, Vila J, Lluch S, Romero FJ, 1994 4-Hydroxynonenal, a lipid peroxidation product, induces relaxation of human cerebral arteries. J.Cereb.Blood Flow Metab 14, 693–696. [PubMed: 8014218]

Matanoski GM, Santos-Burgoa C, Schwartz L, 1990 Mortality of a cohort of workers in the styrene-butadiene polymer manufacturing industry (1943–1982). Environ Health Perspect 86, 107–117. [PubMed: 2401250]

Moyer TP, Charlson JR, Enger RJ, Dale LC, Ebbert JO, Schroeder DR, Hurt RD, 2002 Simultaneous analysis of nicotine, nicotine metabolites, and tobacco alkaloids in serum or urine by tandem mass spectrometry, with clinically relevant metabolic profiles. Clin Chem 48, 1460–1471. [PubMed: 12194923]

Nagata K, Duggan A, Kumar G, Garcia-Anoveros J, 2005 Nociceptor and hair cell transducer properties of TRPA1, a channel for pain and hearing. The Journal of neuroscience : the official journal of the Society for Neuroscience 25, 4052–4061. [PubMed: 15843607]

Nair U, Bartsch H, Nair J, 2007 Lipid peroxidation-induced DNA damage in cancer-prone inflammatory diseases: a review of published adduct types and levels in humans. Free Radic Biol Med 43, 1109–1120. [PubMed: 17854706]

Penn A, Snyder CA, 1996 Butadiene inhalation accelerates arteriosclerotic plaque development in cockerels. Toxicology 113, 351–354. [PubMed: 8901924]

Pozsgai G, Bodkin JV, Graepel R, Bevan S, Andersson DA, Brain SD, 2010 Evidence for the pathophysiological relevance of TRPA1 receptors in the cardiovascular system in vivo. Cardiovasc Res 87, 760–768. [PubMed: 20442136]

Reddy S, Finkelstein EI, Wong PS, Phung A, Cross CE, van der Vliet A, 2002 Identification of glutathione modifications by cigarette smoke. Free Radic Biol Med 33, 1490–1498. [PubMed: 12446206]

Romero FJ, Romero MJ, Bosch-Morell F, Martinez MC, Medina P, Lluch S, 1997 4-hydroxynonenal-induced relaxation of human mesenteric arteries. Free Radical Biology and Medicine 23, 521–523. [PubMed: 9214591]

Schwartz ES, Christianson JA, Chen X, La JH, Davis BM, Albers KM, Gebhart GF, 2011 Synergistic role of TRPV1 and TRPA1 in pancreatic pain and inflammation. Gastroenterology 140, 1283–1291 e1281–1282. [PubMed: 21185837]

Talavera K, Gees M, Karashima Y, Meseguer VM, Vanoirbeek JA, Damann N, Everaerts W, Benoit M, Janssens A, Vennekens R, Viana F, Nemery B, Nilius B, Voets T, 2009 Nicotine activates the chemosensory cation channel TRPA1. Nature neuroscience 12, 1293–1299. [PubMed: 19749751]

Trevisan G, Benemei S, Materazzi S, De Logu F, De Siena G, Fusi C, Fortes Rossato M, Coppi E, Marone IM, Ferreira J, Geppetti P, Nassini R, 2016 TRPA1 mediates trigeminal neuropathic pain in mice downstream of monocytes/macrophages and oxidative stress. Brain 139, 1361–1377. [PubMed: 26984186]

Tuma DJ, Hoffman T, Sorrell MF, 1991 The chemistry of acetaldehyde-protein adducts. Alcohol and alcoholism (Oxford, Oxfordshire). Supplement 1, 271–276.

Voulgaridou GP, Anestopoulos I, Franco R, Panayiotidis MI, Pappa A, 2011 DNA damage induced by endogenous aldehydes: current state of knowledge. Mutat Res 711, 13–27. [PubMed: 21419140]

Wang MY, Chung FL, Hecht SS, 1988 Identification of crotonaldehyde as a hepatic microsomal metabolite formed by alpha-hydroxylation of the carcinogen N-nitrosopyrrolidine. Chem Res Toxicol 1, 28–31. [PubMed: 2979707]

Yanaga A, Goto H, Nakagawa T, Hikiami H, Shibahara N, Shimada Y, 2006 Cinnamaldehyde induces endothelium-dependent and -independent vasorelaxant action on isolated rat aorta. Biol.Pharm.Bull. 29, 2415–2418. [PubMed: 17142974]

Yang BC, Pan XJ, Yang ZH, Xiao FJ, Liu XY, Zhu MX, Xie JP, 2013a Crotonaldehyde induces apoptosis in alveolar macrophages through intracellular calcium, mitochondria and p53 signaling pathways. The Journal of toxicological sciences 38, 225–235. [PubMed: 23535401]

Yang BC, Yang ZH, Pan XJ, Liu XY, Zhu MX, Xie JP, 2013b Crotonaldehyde induces apoptosis and immunosuppression in alveolar macrophages. Toxicol In Vitro 27, 128–137. [PubMed: 23000924]

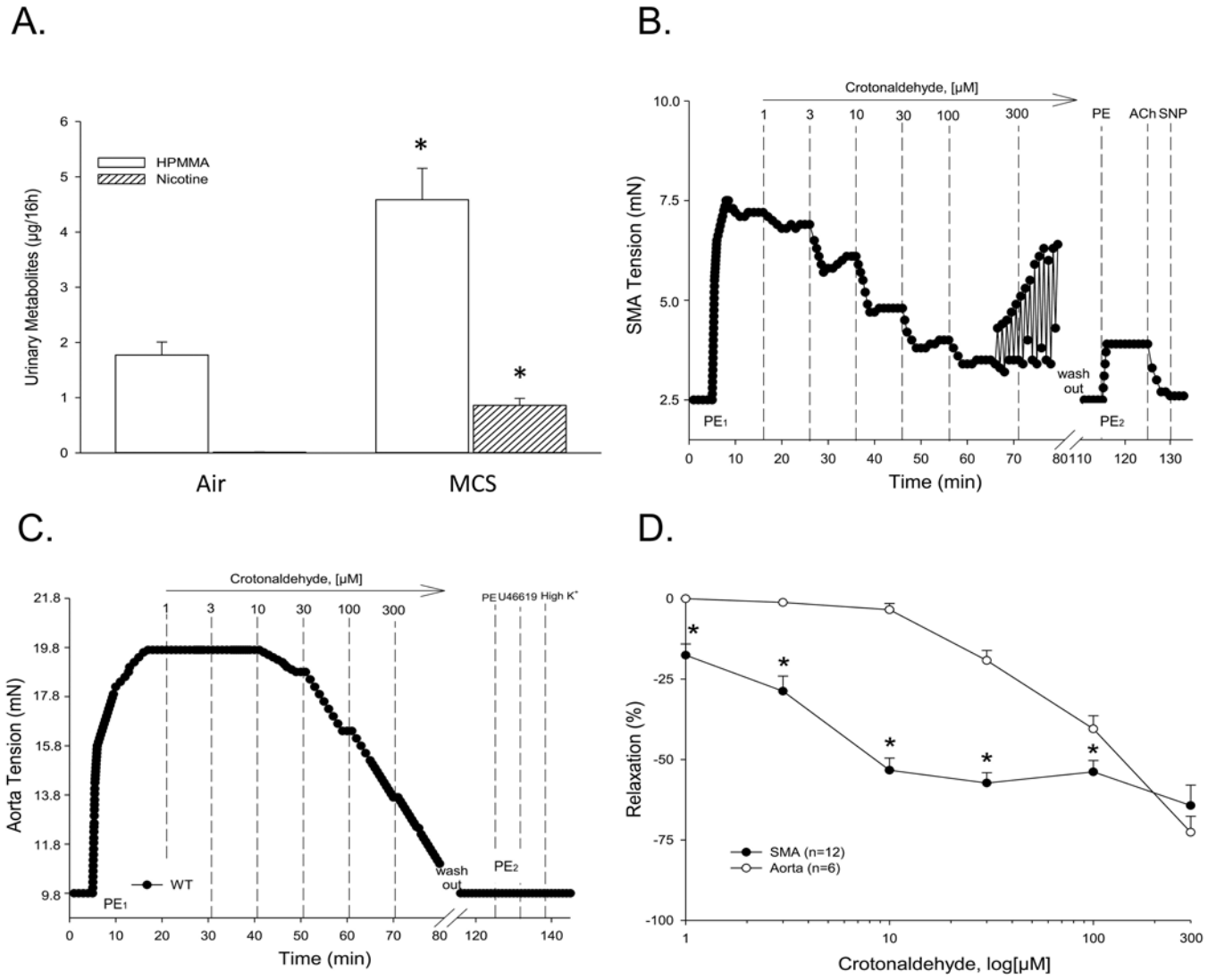

Fig. 1. Crotonaldehyde-induced (CR) relaxation in aorta and SMA.

A) Quantification of mass spectrometry analyses of primary CR metabolite (3-hydroxy-1-methylpropylmercapturic acid; HPMMA) and nicotine in urine of air and mainstream cigarette smoke-exposed (MCS; 12 cigarettes/6 h) male mice 16h post-exposure. (Note: Graph is derived from published data)(Conklin *et al.*, 2018). **B**) Representative trace of CR-stimulated (1–300 µM) relaxation and tension oscillations of phenylephrine (PE) pre-contracted SMA, and post-CR contractility impairment. **C**) Representative trace of CR-stimulated (1–300 µM) relaxation of PE pre-contracted aorta, and post-CR contractility impairment. **D**) Summary data of CR-induced relaxation in PE pre-contracted SMA and aorta. Values = means ± SE of 3–4 preparations. *, $p<0.05$; SMA vs aorta.

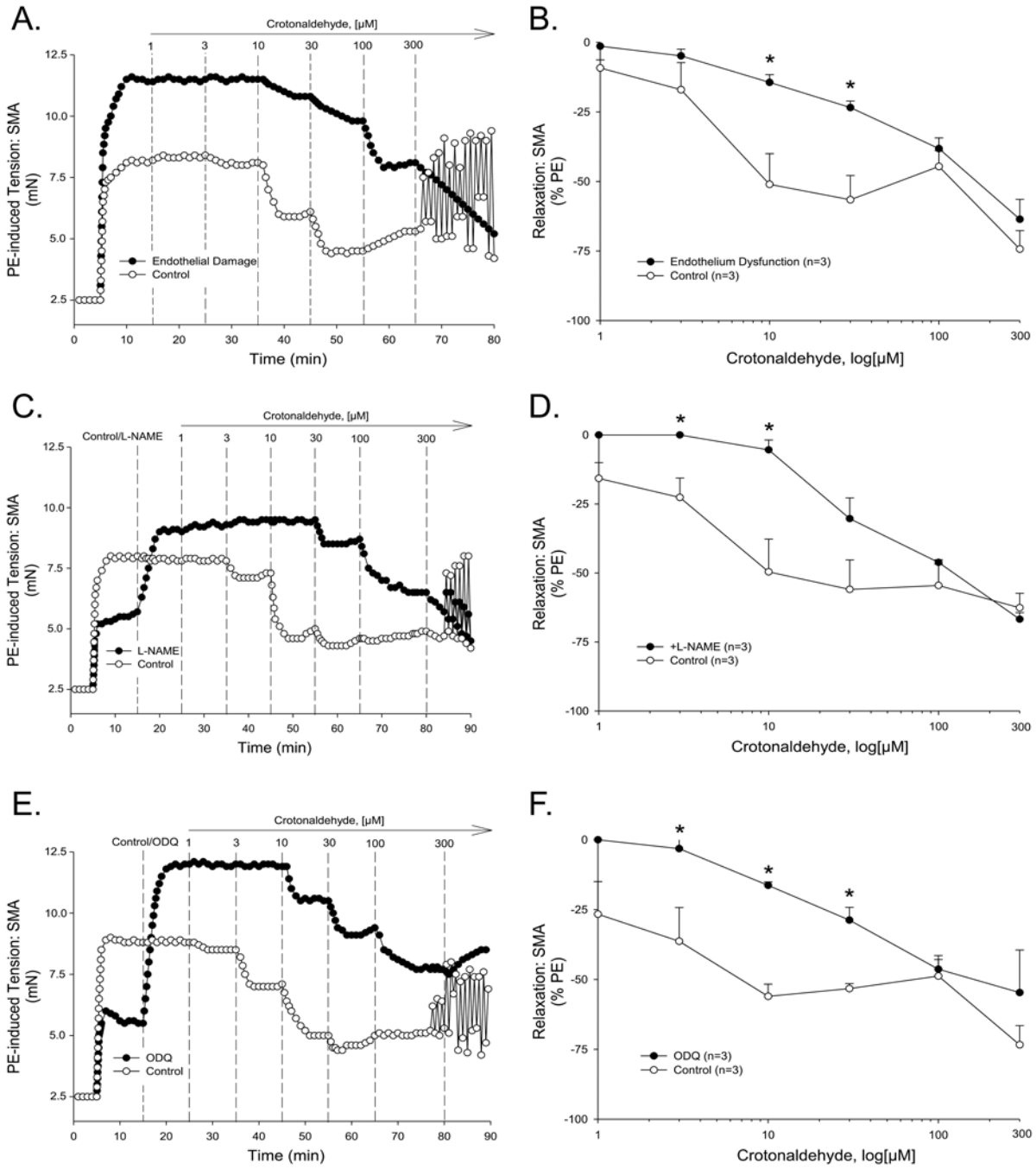

Fig. 2. Mechanisms of CR-induced relaxation in WT SMA.

A) Representative traces and **B**) summary data of CR-stimulated relaxation of PE-induced contraction in WT SMA with and without endothelium impairment due to 5 min of air perfusion. **C**) Representative traces and **D**) summary data of CR-stimulated relaxation of PE-induced contraction in WT SMA with and without L-NAME (100 μM). **E**) Representative traces and **F**) summary data of CR-stimulated relaxation of PE-induced contraction in WT SMA with and without the guanylyl cyclase (GC) antagonist, ODQ (3

μM), added to bath after PE-induced contraction plateaued and prior to cumulative addition of CR. Values = means ± SE of 3–4 preparations. *, $p<0.05$; control vs treatment group.

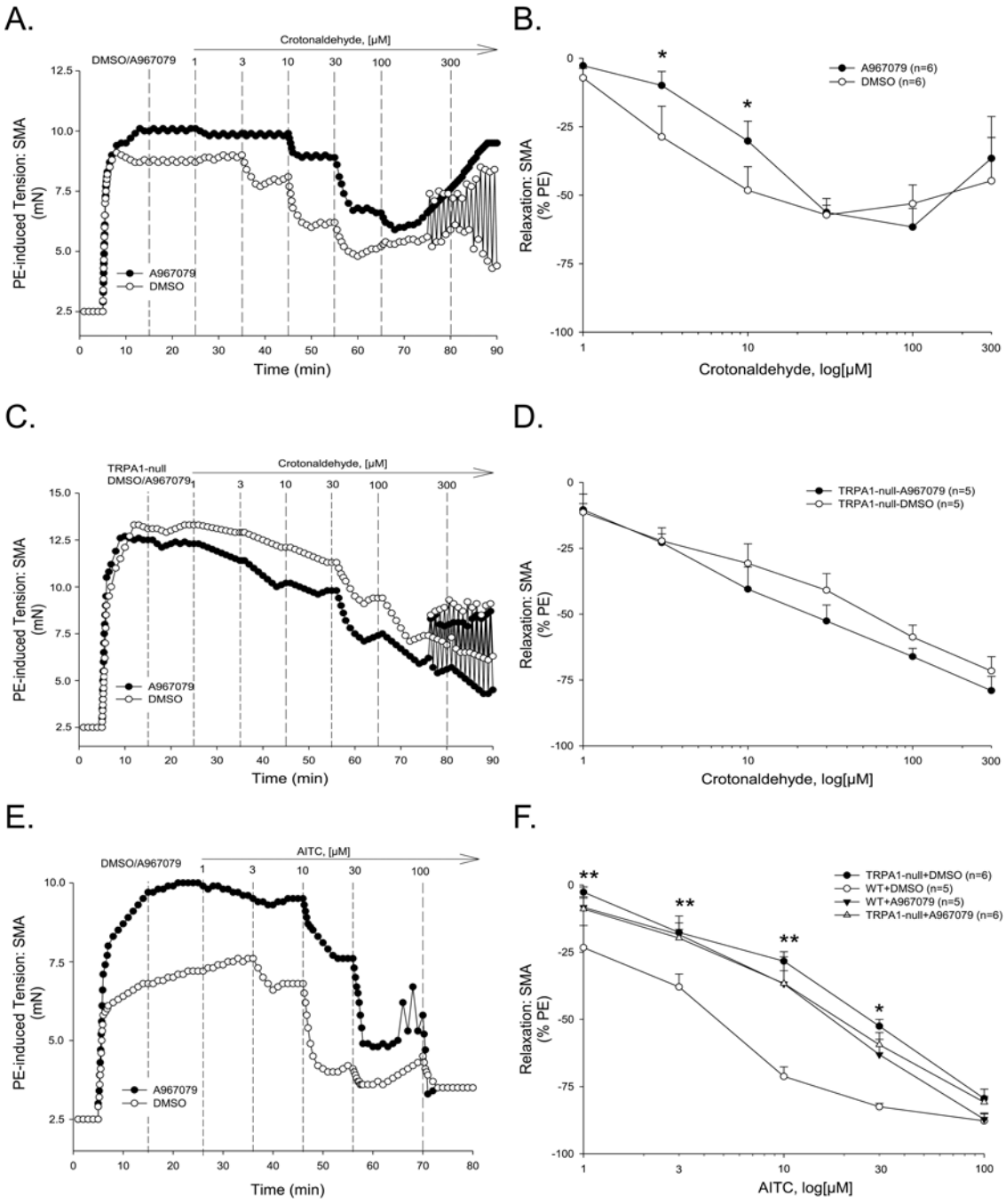

Fig. 3. Role of the TRPA1 channel in CR- and AITC-induced relaxations in SMA.

A) Representative traces and **B**) summary data of CR-stimulated relaxation of phenylephrine (PE) pre-contracted SMA in the absence (control) and presence of the TRPA1 antagonist, A967079 (1 μM) added after PE-induced contraction plateaued and prior to cumulative addition of CR in wild type (WT) SMA. **C**) Representative traces and **D**) summary data of CR-stimulated relaxation of PE pre-contracted SMA of TRPA1-null mice in the presence and absence (control) of the TRPA1 antagonist, A967079 (1 μM) added after PE-induced contraction plateaued and prior to cumulative addition of CR. **E**) Representative traces and

F) summary data of AITC-stimulated, concentration-dependent relaxation of PE-contracted WT and TRPA1-null SMA with (DMSO, vehicle control) or with TRPA1 antagonist, A967079 (1 μM). Values = means ± SE of 3–4 preparations. *, $p<0.05$; control vs treatment group.

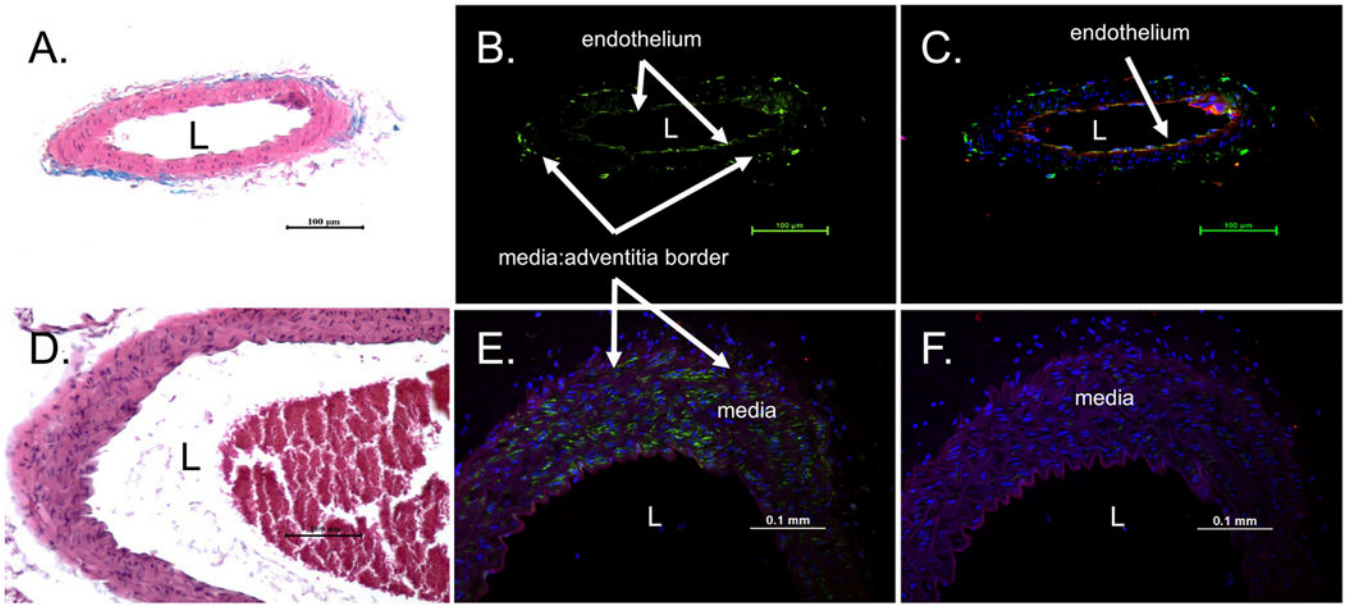

Fig. 4. Localization of TRPA1 in SMA and aorta.

Formalin-fixed, paraffin-embedded, cross-sections of murine WT SMA (**A-C**) and aorta (**D-F**) were stained with H&E (**A, D**) or for immunofluorescent localization of TRPA1 in endothelium and media of SMA (green staining, **B**) or co-localized with endothelial cell marker, isolectin (red staining, endothelium; overlap makes yellow staining) and nuclear staining with DAPI (blue staining, **C**). Immunofluorescent localization of TRPA1 in media of aortic cross-section (green staining, **E**) but not endothelium. **F**) TRPA1 staining of aortic media was blocked by a TRPA1 blocking peptide. Isolectin was used as a marker of endothelium (red staining) and nuclear staining as a cell marker (DAPI, blue). **Abbr.:** L, lumen. All images were taken at 200x magnification (scale bar = 100 μm).

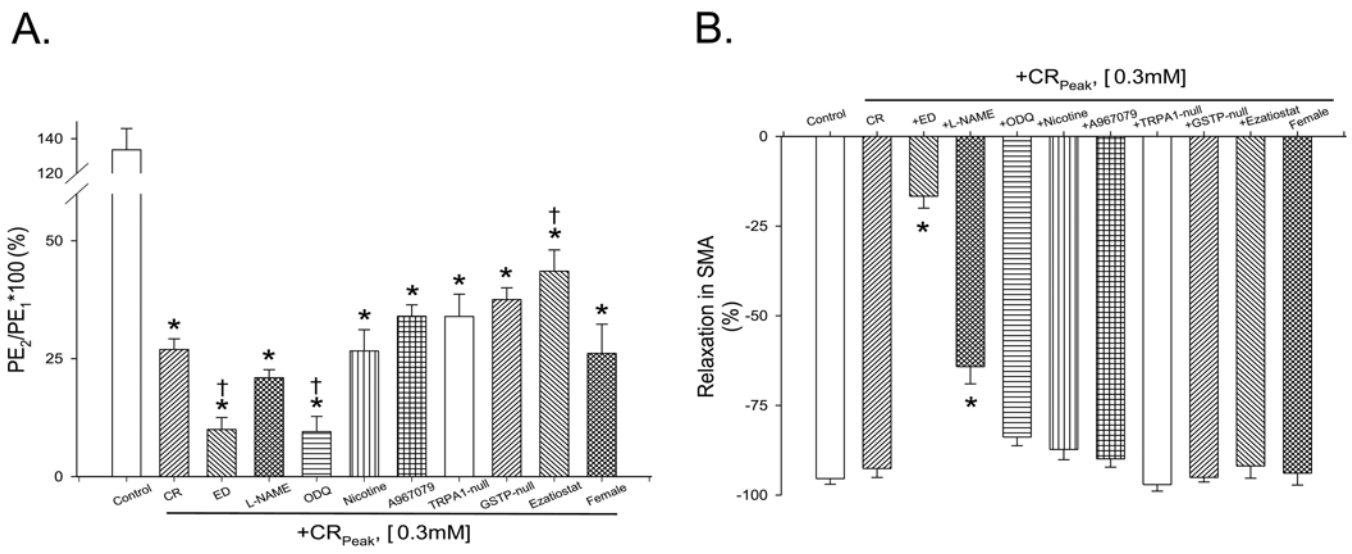

Fig. 5. Impaired contractility (vasotoxicity) of CR exposure in SMA.

After exposure to CR, blood vessels were washed 3x with fresh buffer to remove CR. To test for vasotoxicity, SMA were pre-contracted with and tension recorded (PE_2). **A**) Ratio of PE_2 (PE-induced tension post-CR [300 μM] exposure) to PE_1 (initial PE-induced tension pre-CR) (PE_2/PE_1*100) was quantified and compared across all groups. **B**) Effects of CR on ACh-induced relaxation was quantified and compared across all groups. **Abbr.**: ED, endothelial dysfunction induced by mechanical air perfusion; L-NAME, N^{ω}-nitro-$_L$-arginine methyl ester hydrochloride, 100 μM; ODQ, 1h-[1,2,4]oxadiazolo[4,3-a]quinoxalin-1-one,3 μM; A967079, TRPA1 antagonist, 1 μM; Ezatiostat, 1 μM; Nicotine, 1 μM; (f), female. All SMA were from male mice except where indicated (f). Values = means ± SE of 3–6 preparations. *, $p<0.05$; untreated control vs CR-treated control (B only).

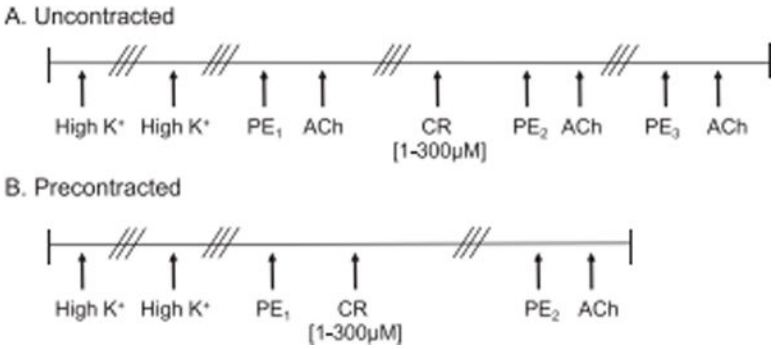

Schematic 1: Protocols for testing CR in uncontracted and precontracted blood vessels.

All blood vessels were stimulated with High K^+ followed by washout (i.e., 3 exchanges of fresh PSS; ///), and process repeated. **A)** Uncontracted blood vessels were then contracted with PE (PE_1) and relaxed with ACh before washout. Uncontracted vessels were then exposed to cumulative CR [1–300 μM] prior to PE (PE_2) and ACh additions. After washout, vessels were stimulated with PE (PE_3) and ACh. **B)** Blood vessels were precontracted with PE (PE_1) followed by cumulative CR [1–300 μM] addition. After washout, vessels were stimulated with PE (PE_2) and ACh. **In both A and B,** the PE_2/PE_1 tension (%) was calculated by dividing PE-induced tension post-CR-exposure (i.e., PE_2) by PE-induced tension pre-CR (i.e., PE_1) and multiplying by 100. In uncontracted blood vessels only, the PE_3/PE_1 tension (%) was calculated by dividing PE-induced tension post-CR-exposure and washout (i.e., PE_3) by PE-induced tension pre-CR (i.e., PE_1) and multiplied by 100. ACh-induced relaxation was calculated as the % reduction in PE-induced tension.

Table 1.

Efficacy (maximal relaxation, E_{max}) of CR-induced relaxations of PE-precontracted superior mesenteric artery (SMA; male and female) with and without inhibitor treatments.

SMA (+treatment)	E_{max} (control, PE+vehicle)	E_{max} (ED or PE+inhibitor)
WT+ED	−74.3±6.6	−63.6±7.1
WT+L-NAME	−62.7±5.3	−66.8±2.4
WT+ODQ	−73.4±6.9	−54.7±15.2
WT+A967079	−57.2±3.5	−61.6±6.8
TRPA1-null+A967079	−70.5±6.4	−79.0±4.2
GSTP-null	−52.6±2.9	--
WT+Ezatiostat	−56.5±7.2	−61.5±2.5
WT+Nicotine	−67.0±4.2	−55.0±6.5$^{\#}$
WT (f)	−59.8±3.9	--

Values = means ± SE. Abbr.: PE, phenylephrine, 10 μM; ED, endothelial dysfunction induced by mechanical air perfusion; L-NAME, N^{ω}-nitro-L-arginine methyl ester hydrochloride, 100 μM; ODQ, 1h-[1,2,4]oxadiazolo[4,3-a]quinoxalin-1-one,3 μM; A967079, TRPA1 antagonist, 1 μM; Ezatiostat, 1 μM; Nicotine, 1 μM; --, experimental group not performed; (f), female. All SMA were from male mice except where indicated (f). n=3–6 per group.

$^{\#}$, 0.05<p<0.10; treatment group vs matched control (PE+vehicle).

Table 2.

The sensitivity (effective concentration inducing 50% relaxation; EC_{50}; in μM) of CR-induced vasorelaxation in PE pre-contracted murine superior mesenteric artery (SMA) in the presence and absence of functional endothelium or selective inhibitors.

SMA (+treatment)	EC_{50} (control, PE+vehicle)	EC_{50} (ED or PE+inhibitor)
WT+ED	5.7±1.0	68.2±13.9 *
WT+L-NAME	6.0±2.0	43.6±17.9 *
WT+ODQ	3.9±1.6	35.3±1.6 *
WT+A967079	7.2±2.3	12.1±2.1 *
TRPA1-null	17.9±7.4	14.1±2.7
GSTP-null	5.9±0.8	--
WT+Ezatiostat	4.3±0.7	4.2±0.6
WT+Nicotine	3.3±0.8	5.7±1.2
WT (f)	6.6±0.3 #	--

Values = means ± SE. Abbr.: PE, phenylephrine, 10 μM; ED, endothelial dysfunction induced by mechanical air perfusion; L-NAME, N^{ω}-nitro-L-arginine methyl ester hydrochloride, 100 μM; ODQ, 1h-[1,2,4]oxadiazolo[4,3-a]quinoxalin-1-one, 3 μM; A967079, TRPA1 antagonist, 1 μM; Ezatiostat, 1 μM; Nicotine, 1 μM; --, experimental group not performed; (f), female. All SMA were from male mice except where indicated (f). n=3–6 per group.

*, $p<0.05$; treatment (PE+inhibitor) vs matched control (PE+vehicle).

#, $p<0.05$; female WT vs male WT (control group).

Table 3.

Characteristics of tension oscillations (spasms) induced by a high concentration of CR (300 μM) in PE-precontracted SMA.

SMA (+treatment)	Frequency (oscillations/min)	Amplitude (mN)	Duration (s)
WT+CR	2.0±0.4	2.0±0.3	28.4±5.6
WT+CR+ED	0*	--	--
WT+CR+L-NAME	1.3±0.2	0.9±0.1	37.5±4.8
WT+CR+ODQ	2.1±0.6	1.2±0.5	28.8±5.1
WT+CR+A967079	1.7±0.3	1.9±0.5	23.3±2.0
TRPA1-null+CR	1.7±0.3	2.0±0.2	28.3±2.0
GSTP-null+CR	1.9±0.6	3.4±0.5	23.6±3.5
WT+CR+Ezatiostat	1.9±0.1	2.1±0.2	24.4±1.3
WT+Nicotine	1.8±0.2	1.6±0.3	17.7±4.1
WT (f) +CR	1.4±0.6	2.9±0.6	29.5±4.9

Values = means ± SE. Abbr.: PE, phenylephrine, 10 μM; WT, wild type; ED, endothelial dysfunction; --, no data to measure; L-NAME, N^{ω}-nitro-L-arginine methyl ester hydrochloride, 100 μM; ODQ, 1h-[1,2,4]oxadiazolo[4,3-a]quinoxalin-1-one, 3 μM; A967079, TRPA1 antagonist, 1 μM; Ezatiostat, 1 μM; Nicotine, 1 μM; (f), female. All SMA were from male mice except where indicated (f). n=3–10 per group.

*, $p<0.05$; treatment vs control group (WT+CR).

Table 4.

Effects of CR on contractility (vasotoxicity) and endothelial-dependent relaxation in SMA.

SMA (+treatment)	PE_2/PE_1 (%)	ACh (%)
WT (control)	133.6±12.3	−95.4±1.6
WT+CR	27.0±2.2 *	−92.6±2.5
WT+CR+ED	10.0±2.5 *†	−16.7±3.3 *
WT+CR+L-NAME	21.0±1.7 *	−64.2±4.8 *
WT+CR+ODQ	9.5±3.2 *†	−83.9±2.4
WT+CR+A967079	34.0±2.4 *	−89.9±2.3
TRPA1-null+CR	34.0±4.7 *	−97.1±1.8
GSTP-null+CR	37.5±2.5 *	−95.1±1.3
WT+Ezatiostat	43.5±4.5 *†	−91.9±3.4
WT+CR+Nicotine	26.6±4.5 *	−87.3±2.9
WT (f) +CR	26.1±6.2 *	−93.9±3.3

Values = means ± SE. Abbr.: PE, phenylephrine, 10 μM; ACh, acetylcholine chloride, WT, wild type; ED, endothelial dysfunction; L-NAME, N^{ω}-nitro-L-arginine methyl ester hydrochloride, 100 μM; ODQ, 1h-[1,2,4]oxadiazolo[4,3-a]quinoxalin-1-one, 3 μM; A967079, TRPA1 antagonist, 1 μM; Ezatiostat, 1 μM; Nicotine, 1 μM, (f), female. The PE_2/PE_1 tension (%) was calculated by dividing PE-induced tension post-CR-exposure (PE_2) by PE-induced tension pre -CR (i.e., PE_1) and multiplied by 100. ACh-induced relaxation was calculated as the % reduction in PE_2-induced tension. All SMA were from male mice except where indicated (f). n=3–10 per group.

*, $p<0.05$; treatment group vs WT group (male, control).

†, $p<0.05$; treatment group vs WT+CR group.